Chapter 3:

Generation of strains for study of kinetochore genes

3. Chapter 3: Generation of strains for study of kinetochore genes

3.1. Analysis of DASH complex proteins in *M. oryzae*

3.1.1 Homology based identification of Dam1 complex proteins using *Magnaporthe oryzae* genome sequence

The orthologues of *S. cerevisiae* and *S. pombe* DASH complex proteins were identified in *M. oryzae* using BLASTP. For comparison I considered the four organisms where the complex has been characterised previously, *S. cerevisiae, S. pombe, C. albicans and C. neoformans* (Table 3.1). The filamentous fungus *N. crassa* was also included in the analysis. The DAM1/DASH complex domain is an approximately 55-70 amino acid stretch that is characteristic of the members of this complex. All *M. oryzae* proteins carried the characteristic DASH complex domain.

At the gene level, many of the *M. oryzae* genes showed long intronic regions, in some cases distributed over multiple introns (Table 3.1). Further, Dad1, Dad3, Dad4, Duo1, Hsk3 and Spc34 transcripts have been reported to have 5' and/or 3'UTRs probably involved in regulation at the transcript level. MoDam1, like *S. pombe* Dam1, did not show a strong propensity to form coiled coil domains as seen in *S. cerevisiae* and *C. albicans*. In *S. cerevisiae*, Dam1, Duo1, Dad2, Dad4, Hsk3, Spc19 and Spc34 form coiled coil domains. Such domains are common among structural proteins, cytoskeleton proteins or those involved in oligomerisation. ScDam1 and ScDuo1 display several cross links within the coiled coil regions (Legal et al., 2016). Further, owing to the α-helix structure, Hsk3, Dad2 and Dad4 display multiple interactions within these regions and display a coiled coil structure rather than a globular form. Spc19 shows cross links between the two coiled coil regions, suggesting that the coil may be involved in the formation of an antiparallel dimer (Legal et al., 2016). *Magnaporthe* Dad2, Dad4, Duo1, Hsk3, Spc19 and Spc34 proteins were predicted to have coiled coil domains (Table 3.1).

Protein	Hits based on *S. cerevisiae* & *S. pombe* proteins	Chr	Gene Size (bp)	Protein size (aa)	Coiled Coils	Protein size (aa) (% similarity)				
						S. cerevisiae	*C. albicans*	*S. pombe*	*C. neoformans*	*N. crassa*
Ask1	MGG_07143	2	1380	459	-	292 (27)	594 (33)	307 (30)	617 (27)	487 (60)
Dad1	MGG_12092	6	930	99	-	94	90	90	106	137
Dad2	MGG_02522	1	521	145	Yes	133	125	94	129	130
Dad3	MGG_06996	1	1179	107	-	94	138	86	112	119
Dad4	MGG_16761	3	1044	72	Yes	72	72	72	72	72
Dam1	MGG_00874	5	805	220	-	343 (22)	277 (25)	155 (37)	121 (26)	248 (65)
Duo1	MGG_02484	1	1819	225	Yes	247	171	282	431	324
Hsk3	MGG_15008	7	1371	99	Yes	69	106	94	90	156
Spc19	MGG_09127	SC 8	642	184	Yes	165	175	152	190	194
Spc34	MGG_00887	5	2476	263	Yes	295	247	164	-	253

Table 3.1: DASH complex proteins in *M. oryzae.*

The loci coding for all ten members of DASH complex proteins in *M. oryzae* homologous to *S. cerevisiae* and *S. pombe* are listed. The details of Ask1 and Dam1 are highlighted. The table provides the protein and gene sizes and % similarity to previously characterised fungal proteins.

For this study, I focussed on Dam1 (MGG_00874) and Ask1 (MGG_07143). Ask1 interacts directly with Dam1 in *S. cerevisiae.* It is the largest protein of the complex in most fungi including *M. oryzae,* except for *S. cerevisiae* where Dam1 is the largest. Both these proteins show considerable size variation. While *S. cerevisiae* Dam1 is 343 amino acids long, *Cryptococcus neoformans* Dam1 protein has only 121 amino acids. The *M. oryzae* Dam1 protein lies in between with 220 amino acids (Table 3.1). With respect to Ask1, *S. cerevisiae* has the smallest protein with 292 amino acids, while *C. neoformans* Ask1 is more than twice as large, at 617 amino acids. The *M. oryzae* Ask1 and Dam1 proteins are more closely related to those of the filamentous fungus *N. crassa* than to the yeast proteins (60% and 65% sequence similarity respectively) (Table 3.1).

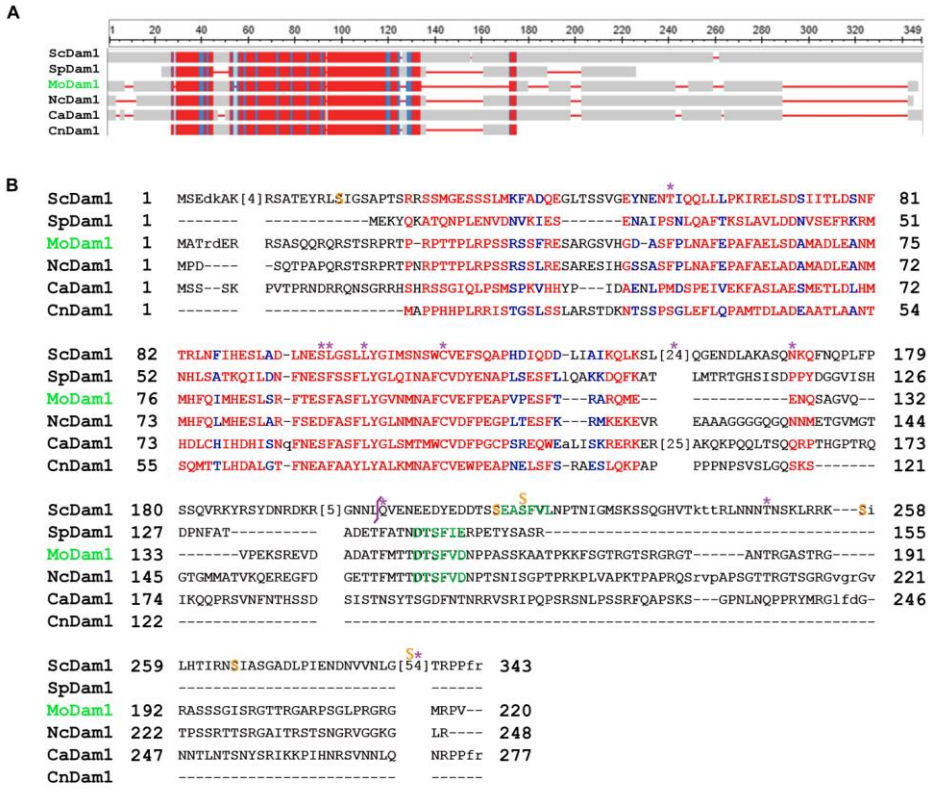

Figure 3.1: Multiple sequence alignment of Dam1 proteins

A) Alignment of 6 fungal Dam1 proteins using Constraint-based multiple sequence alignment tool (COBALT) to define conserved regions. Red indicates conserved residues (within the constraints placed), blue indicates columns without gaps and grey columns carry gaps. B) Multiple sequence alignment shown in A) at amino acid level. Numbers indicate amino acid position and colour code is the same as in A). Columns with less than 50% sequences showing gaps are indicated in upper case, more than 50% gaps are indicated by lower case. The amino acid residues marking the Plo1 consensus sequences are shown in green. The serine residues phosphorylated by Ipl1 (S20, S257, S265, S292), Mps1 (S218, S221) and Cdk1 (S216, S250) in *S. cerevisiae* are marked in orange. Asterisks indicate sites altered in *S. cerevisiae* Dam1 mutants *dam1-1* (C111Y), *dam1-5* (T58I, L98P, N139S, T332A), *dam1-9* (S97F, N139S, K170E, S328 P, T332A), *dam1-10* (L102S, C111R, N139S, T249I, N302D, T332A, I336Stop), *dam1-11* (L98P, N139S, T332A) and *dam1-19* (Q205STOP) described previously (Jones et al. 2001, Cheeseman et al., 2001).

The DASH complex domain lies towards the N-terminus of the *M. oryzae* Dam1 protein extending from amino acids 57-112 (Figure 3.1A).

Although the overall Dam1 protein sequence similarity is ~25-35% (Table 3.1), the DASH complex domain of *M. oryzae* Dam1 shows much higher similarity, 60.7% with *S. cerevisiae* and 58.9% with *S. pombe* compared to 49.2% between the two yeasts. The *M. oryzae* Dam1 protein shows features of both *S. pombe* and *S. cerevisiae* (Fig. 3.1A, B). Like *S. cerevisiae*, the filamentous fungi have a 50-60 amino acid N-terminal region before the DASH complex domain, which is much smaller in *C. neoformans* and *S. pombe*. The N and C-terminal regions of *M. oryzae* Dam1 beyond the DASH complex domain showed a propensity for disorder due to the presence of polar amino acids contributing to low complexity regions.

The Dam1 protein C-terminus makes a major contribution to protein size variation between different fungal Dam1 proteins, with *S. cerevisiae* showing one of the longest C-terminus regions (Figure 3.1B). Interestingly in *S. cerevisiae* it is this C-terminus which is crucial for interaction with Duo1, Ask1 and the tubulin dimers and it also carries the important Ipl1 (AuroraB kinase in humans) phosphorylation sites that regulate the attachment/detachment to microtubules.

Most of this critical region is absent in *S. pombe* and partially present in filamentous fungal proteins. Many of the Duo1-interacting residues as well as residues required for interaction of *S. cerevisiae* Dam1 from individual decamers are concentrated between amino acids 240-330, a region that is unique to ScDam1, and absent in other fungi including *M. oryzae* (Fig. 3.1A, B). Thus, different interactions may come into play during complex assembly in the other fungi. The Polo kinase phosphorylation sites/motifs were predicted in *Magnaporthe* Dam1 at positions 150-155 (Fig. 3.1B).

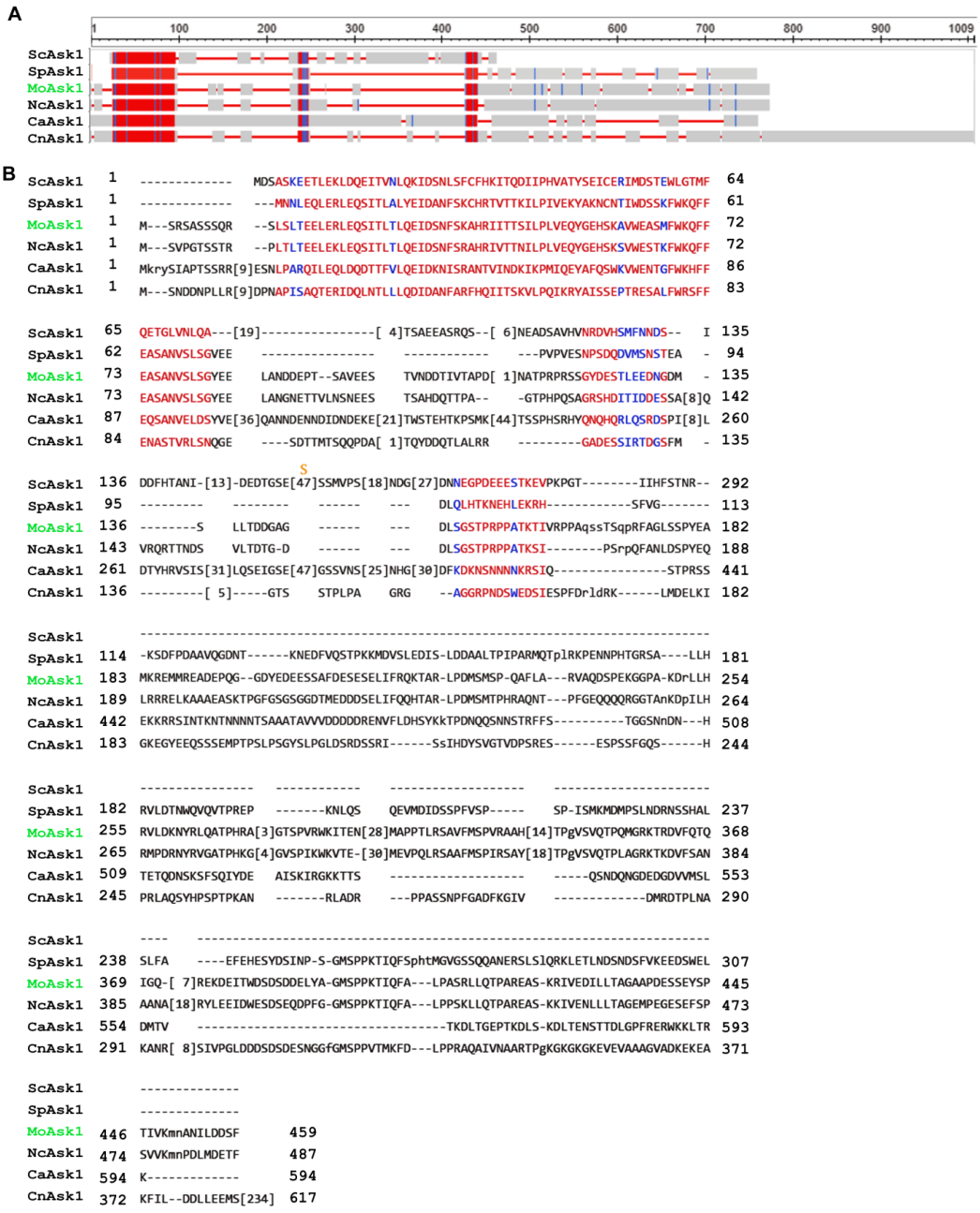

Figure 3.2: Multiple sequence alignment of Ask1 proteins

A) Alignment of 6 fungal Ask1 proteins using Constraint-based multiple sequence alignment (COBALT). Red indicates conserved residues (within the constraints placed), blue indicates columns without gaps and grey columns carry gaps. B) Multiple sequence alignment. Numbers indicate amino acids. Columns with less than 50% sequences showing gaps are indicated in uppercase, more than 50% gaps are indicated by lowercase. The phosphorylation site (Li et al. 2003/2005) is marked in orange (S200).

In Ask1, the DASH complex domain was present towards the N-terminal region (Fig. 3.2A, B). The C-terminus of Ask1 proteins was far more variable in length and sequence, suggesting specialised functions in the different fungi. A 250 amino acid long stretch, present at the C-terminus of *C. neoformans* Ask1 was unique and not found in either of the other five ascomycete yeasts or filamentous fungi (Fig. 3.2). It would be interesting to see whether this is a feature of basidiomycete Ask1 proteins or specific to *C. neoformans*.

I compared the Dam1 and Ask1 proteins across a larger fungal group (budding, fission and dimorphic yeasts and filamentous fungi) that is more diverse in cell growth and division patterns, nature of centromeres (point and regional), structure of nuclear envelope during mitosis (closed, semi-open, semi-closed), host specificity (plant, animal and human), chromosome number, genome size, nuclear organisation (uninucleate and multinucleate cells), number of MTs per kinetochore and KT clustering (Figs. 3.3, 3.4). The information available regarding many of the above characteristics is restricted to a few groups and *M. oryzae* proteins are fairly distant from any of the well studied fungal classes (Fig. 3.3). Further the fungal Dam1 and Ask1 proteins showed a different pattern of phylogenetic clustering.

In case of Dam1 all the basidiomycete proteins clustered together as one clade closely related to yeast proteins, while the basidiomycete Ask1 proteins were split into two separate clades, one clustered with the yeasts and the other with filamentous fungi. There was minor variation in the Dam1 and Ask1 sequences even between *M. oryzae* strains that clustered together as one clade. The *M. oryzae*, *N. crassa* and *Aspergillus* Dam1 proteins were more closely related to yeast proteins than to the other plant pathogens of the *Fusarium* (*or Gibberella*) and *Colletotrichum* genera. Interestingly, *A. nidulans* Dam1 clustered with the yeast proteins in a clade distant from the other *Aspergillus sps.* The *M. oryzae*, *P. anserina*

and *N. crassa* Ask1 proteins clustered close together with plant pathogens *Fusarium, Gibberella, Botrytis* and *Colletotrichum* genera.

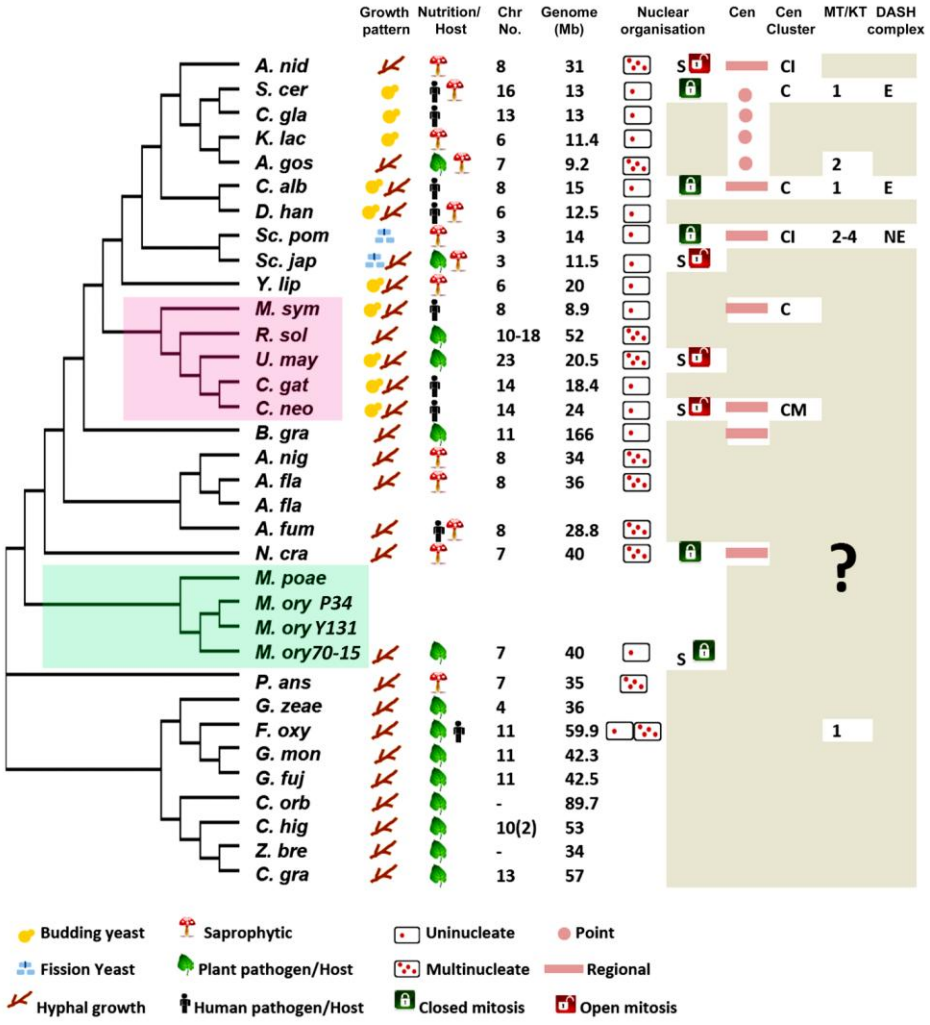

Figure 3.3: Phylogenetic tree of fungal Dam1 proteins

Unrooted phylogenetic tree (cladogram) of Dam1 proteins from a variety of fungal species is shown. The panel on the right includes details of growth patterns, host, chromosome number, genome size, nuclear organisation, nuclear envelope integrity during mitosis, centromere structure, centromere clustering pattern, number of MTs per kinetochore and requirement of DASH complex proteins in these fungi. The key at the bottom explains the symbolic representation used in the panel. The *Magnaporthe* proteins are highlighted in the green box. The pink box indicates basidiomycetes. The rest are all ascomycetes.

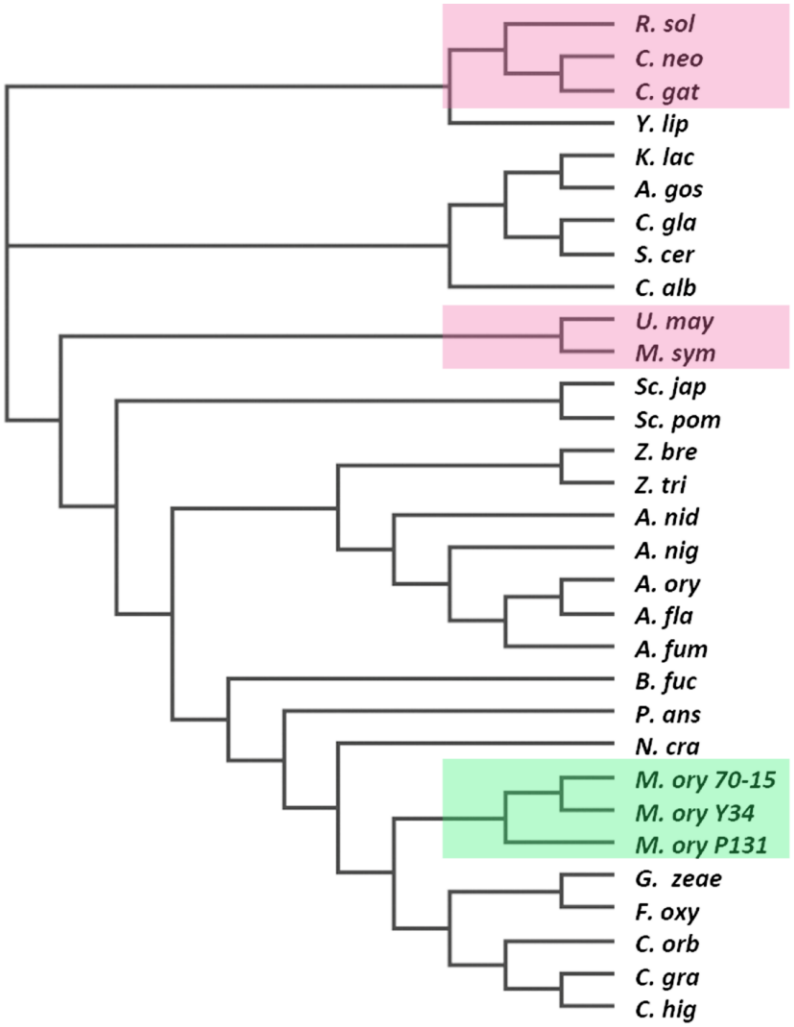

Figure 3.4: Phylogenetic tree of fungal Ask1 proteins

Unrooted phylogenetic tree (cladogram) of Ask1 proteins from a variety of fungal species is shown. The *Magnaporthe* proteins are highlighted in the green box. The pink box indicates basidiomycetes. The rest are all ascomycetes.

I used two approaches to study these kinetochore genes in *M. oryzae*. The first was to study localisation patterns of the proteins during the different developmental stages and the other was to study the effect of gene loss on the development and virulence of the fungus. I also studied the effect of the mutations on mitosis during these developmental stages. In order to do so, I developed a number of strains as described below.

3.2. Development of strains for study of kinetochore proteins in *M. oryzae*

3.2.1 Tagging of genes for localisation studies

Magnaporthe oryzae strain B157 is used as the wild-type background strain for this study and is henceforth referred to as WT. To visualise *M. oryzae* chromosomes and nucleus, histone H1-mCherry tagged strain was developed. The strain was generated by Sulfonylurea Resistance Reconstitution (SRR), a strategy that improves the efficiency of site specific integration. The SRR vector pFGL959-hH1mCherry, derived from the pFGL959 plasmid (a kind gift of pFGL959 plasmid; (Yang and Naqvi, 2014)) (Fig. 3.5A). pFGL959 carries a nuclear mCherry (ccg1 promoter: hH1-mCherry) (Yang and Naqvi, 2014). This expression cassette has been used in several *Magnaporthe* studies to monitor the nucleus. SRR involves site specific integration of the expression construct downstream of the ILV2 locus. The pFGL959-hH1mCherry plasmid was transformed into wild type (WT) *M. oryzae* strain B157 by ATMT (Fig. 3.5A). The 24 chlorimuron ethyl (sulfonylurea) resistant transformants were screened by fluorescence microscopy of conidia to identify transformants showing the characteristic three nuclear spots per conidium, with one spot per cell (Fig. 3.5B).

The SRR strategy efficiently promoted targeted integration with 22 transformants (91% of resistant transformants) showing the desired nuclear pattern. This efficiency of true transformants is much higher than normally observed in *Magnaporthe*, where ectopic intregration is common due to predominance of non-homologous end-joining repair pathway (NHEJ). Seven of the randomly selected microscopy-positive transformants were checked by southern hybridisation and all were confirmed to have the expected pattern (Fig. 3.5C).

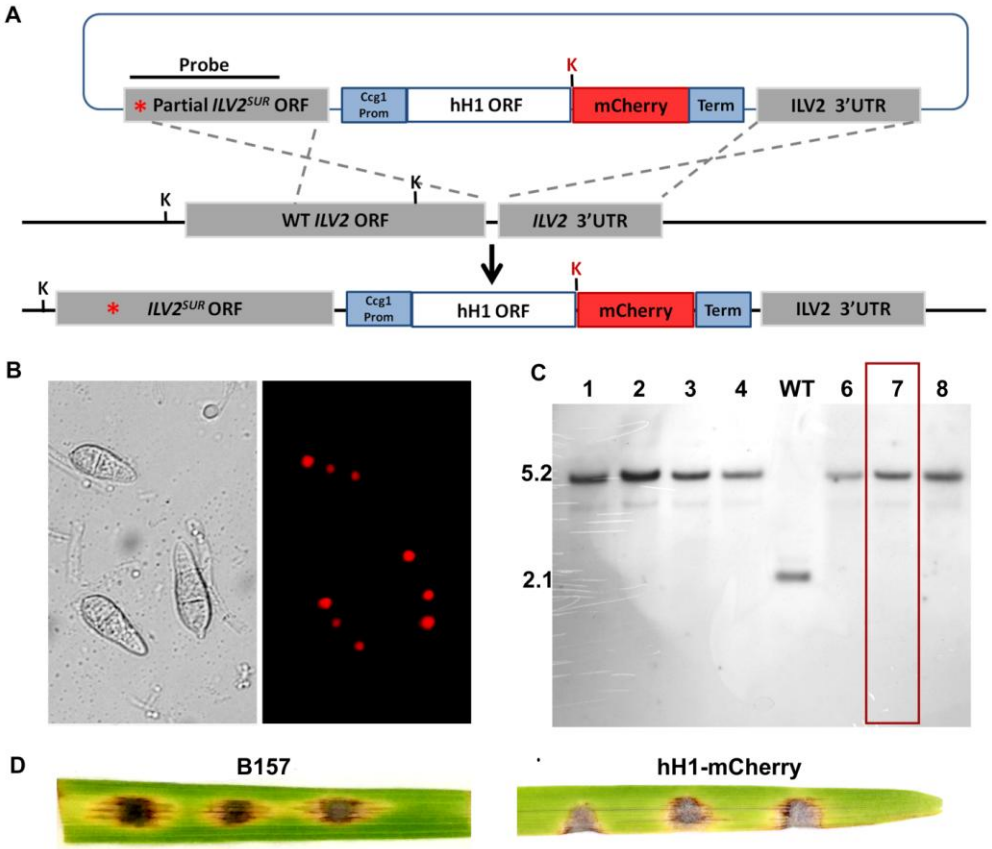

Figure 3.5: Generation of hH1-mCherry tagged strain by SRR

A) Schematic diagram shows histone *hH1-mCherry* construct inserted at the *ILV2* locus by Sulfonylurea resistance reconstitution (SRR) strategy. B) Microscopic screening visualisation of the histone H1 tagged transformants by epifluorescence microscopy. C) Southern hybridisation was used to confirm single copy site-specific integration of *hH1-mCherry* construct. The difference in DNA fragment sizes between the WT (2.1kb) and *hH1-mCherry* (5.2kb) transformants confims correct integration at the native *ILV2* ORF shown in A). Genomic DNA from WT strain and *hH1-mCherry* transformants was digested with KpnI, sites indicated as K in A), and probed with a fragment comprising a part of the *ILV2* locus marked in A). D) Pathogenicity assessment using drop inoculation of WT B157 strain and *H1-mCherry* tagged strains on detached barley leaves. The disease outcome was imaged 5 days post inoculation.

Plasmid construction and generation of tagged strains

Marker fusion tagging (MFT) was used to study localisation of Ask1 and Dam1, where the selectable marker gene, a gene encoding GFP/DsRed

and the gene of interest are expressed as a single fusion protein under a promoter of choice (Lai et al., 2010). For this study, tagged kinetochore protein coding genes were integrated at their native/endogenous genomic loci, such that the native locus was replaced with the tagged one by homologous recombination, and expressed under the native promoter of the gene of interest.

I developed a variety of constructs that would allow the study of localisation of Dam1 with respect to other cellular components, namely chromosomes, microtubule network, inner/middle kinetochore, and other DASH complex members. Constructs were made for GFP- as well as DsRed-tagged versions of *DAM1*. To ensure Dam1 tagging without affecting its function, since both ends of Dam1 are involved in interaction and complex formation, both N-terminal as well as C-terminal constructs were made for Dam1. While for N-terminal tagging I made use of the marker fusion tagging (MFT) technique, the classical tagging approach was used for the C-terminal. Further, to obtain higher fluorescence intensity to aid visualisation of dynamic changes in localisation 2X/3XGFP tagging constructs were also made. All constructs were developed for in-locus integration to replace the native Dam1 gene with the tagged one. In addition to Dam1, constructs were also made for C-terminal tagging of Ask1, also a DASH complex subunit, with GFP and DsRed.

Generation of DsRed/GFP-tagged Dam1 strains

For N-terminal tagging of Dam1 with DsRed, the ~1kb upstream promoter region of *DAM1* was amplified using primers Dam1ProF/Dam1ProR from B157 genomic DNA. The list of all primers used in the study is provided at the end of this chapter (Table 3.3). The ~1kb upstream region was digested with EcoRI/SpeI and cloned into pFGL557 to obtain p557-Dam1Pro. The *DAM1* ORF and 3' flanking region (1052 bp) was amplified from genomic DNA.

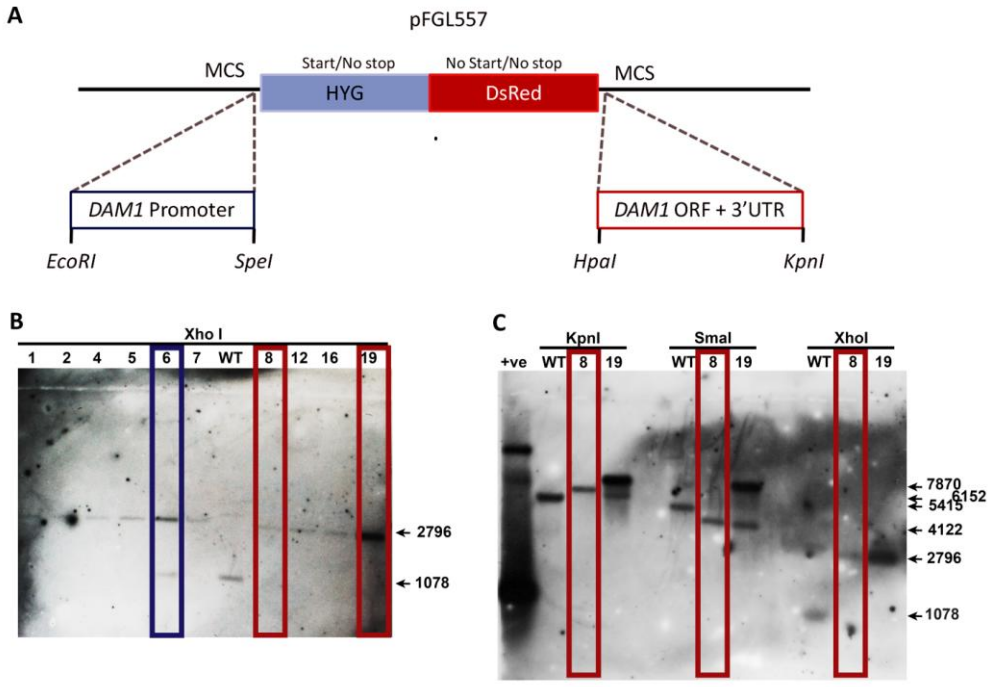

Figure 3.6: Generation of *DsRed-DAM1* tagged strains

A) Schematic diagram shows the construct used for the replacement of the native *DAM1* locus with N-terminal DsRed-tagged *DAM1* by marker fusion tagging. B) Southern hybridisation of genomic DNA, digested with XhoI, shows difference in fragment sizes between WT (1.078 kb) and *DsRed-DAM1* transformants (2.796 kb) consistent with correct integration at the native locus when probed with a fragment. C) Representative Southern hybridisation for a couple of transformants seen in B) with additional restriction enzymes KpnI (WT: 6.152 kb, *DsRed-DAM1*: 7.87 kb) and SmaI (WT: 5.415 kb, *DsRed-DAM1*: 4.122 kb).

The Dam1-ORF-F/Dam1-3UTR-R primers were used in this PCR reaction. It was digested with HpaI/KpnI and cloned in p557-Dam1Pro to give p557-RFPDam1 (Fig. 6A). The clones were confirmed by restriction enzyme digestion and PCR. The plasmids were transformed into *M. oryzae* WT strain B157 by ATMT and selected for hygromycin resistance. The resistant transformants were screened by PCR and confirmed by Southern hybridisation (Fig. 3.6B, C).

To tag Dam1 with GFP on the N-terminus (Fig. 3.7), the *DAM1* 5' flanking region (comprising the promoter) was amplified from B157

genomic DNA using the Dam1-Pro-F/Dam1-Pro-R primer combination. The PCR product was ligated to pFGL718 at EcoRI/SpeI upstream of BAR-GFP to obtain p718-Dam1Pro. Amplification of a 1052bp fragment comprising the *DAM1* ORF and downstream flanking region was carried out using Dam1-ORF-F/Dam1-3UTR-R primers and ligated in frame with BAR-GFP to obstain p718-GFPDam1 (Fig. 3.7A).

In view of the low fluorescence intensity observed in case of DsRed-Dam1 transformants, and a previous study in *S. pombe* which used 3X/4X GFP tags to visualise DASH complex subunits (Gao et al., 2009), a 3XGFP-Dam1 construct was also developed. Transformation was first attempted with the GFP-Dam1 construct by ATMT in the WT B157 strain as well as h1-mCherry tagged strain. Glufosinate (bialaphos) resistant transformants were screened by PCR and confirmed by Southern hybridisation (Fig. 3.7B). The transformants with single in-locus GFP-DAM1 integration were used for further analysis (Fig. 3.7C).

For C-terminal tagging of Dam1, a ~500 bp region of the Dam1 3' flanking region was amplified using primers Dam13UTRF-H3/ Dam13UTRR-Pvu1 from B157 gDNA. It was digested with HindIII/PstI and cloned into pFGL758 to obtain p758-Dam1Dn. The ~1.3kb region of the DAM1 promoter and ORF was amplified using primers Dam15UTR-ER1/Dam1cdsR-Sm1 from genomic DNA. It was digested and cloned in p758-Dam1Dn at EcoRI/SmaI to give p758-Dam1mCherry.

The clones were confirmed by restriction enzyme digestion. Transformation was attempted several times; however it yielded very few resistant transformants, with no true transformants. I reasoned that the C-terminal tag might in some way be interfering with the normal function of the protein and did not pursue this further. Hence, the Dam1 localisation patterns described in this study are all based on the N-terminal GFP-Dam1 (1X GFP) tagged strains.

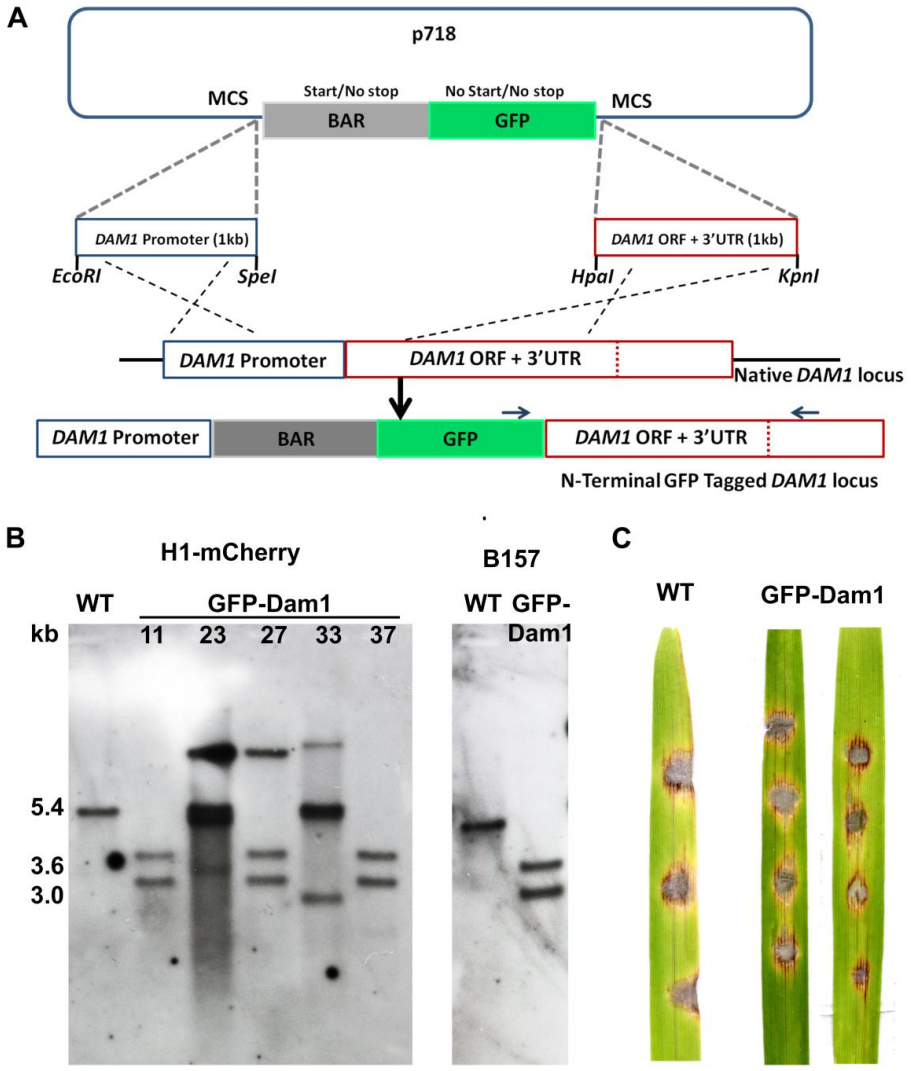

Figure 3.7: Generation of *GFP- DAM1* tagged strains

A) Schematic diagram demonstrates the marker fusion tagging strategy used for the replacement of the native *DAM1* locus with N-terminal GFP-tagged *DAM1*. B) Southern hybridisation of genomic DNA, digested with SmaI, shows difference in fragment sizes between WT (5.4 kb) and *GFP-DAM1* transformants (3 and 3.6 kb) consistent with correct integration at the native locus when probed with a fragment shown in A). Transformants with single copy integration were used for further analysis. C) Pathogenicity assay using drop inoculation of WT and *GFP-DAM1* tagged strains on detached barley leaves. The disease outcome was imaged 5 days post inoculation.

Generation of DsRed/GFP-tagged Ask1 strains

For C-terminal tagging of Ask1, amplification of the 3' region of *ASK1* ORF (1kb) was performed from B157 genomic DNA with primers Ask1tagcdsF-ER1/Ask1tagcdsR-Spe1. It was digested with EcoRI/SpeI and ligated to pFGL557 to obtain the p557-Ask1Up plasmid. The 1kb region of the *ASK1* 3' flanking region was amplified from genomic DNA using primers Ask1stop3UTRF-Hpa1/Ask13UTRR-KpnI. It was digested with HpaI and KpnI and cloned into p557-Ask1Up developed above to give the final p557-Ask1RFP plasmid (Fig. 3.8A). The clones were confirmed by digestion with restriction enzymes. The plasmid was transformed into *M. oryzae* by ATMT and selected for hygromycin resistance. The resistant transformants were screened by PCR and confirmed by Southern hybridisation for site specific single integration (Fig. 3.8B).

For development of Ask1-2XRFP construct, first the 1kb region of the 3' end of the *ASK1* ORF was amplified from B157 genomic DNA using primers Ask1tagcdsF-ER1/Ask1tagcdsR-Spe1, digested with EcoRI/SpeI and ligated with pFGL687 to get the intermediate plasmid p687-Ask1Up. Then, the DsRed ORF of ~700 bp region with ~1 kb *ASK1* 3'UTR was amplified using primers RedF-XmI/Ask13UTRR-KpnI from p557-Ask1RFP (developed earlier, Fig. 3.8A). It was digested with XmaI/KpnI and cloned into p687-Ask1Up at XmaI/KpnI to obtain p687-Ask12XRFP, which was verified by restriction enzyme digestion. (Fig. 3.8C).

Meanwhile, for C-terminal tagging of *ASK1* with GFP (Fig. 3.9), amplification of a fragment comprising ~1kb region from the *ASK1* ORF (3' region) was carried out using B157 genomic DNA as template and Ask1tagcdsF-ER1/ Ask1tagcdsR-Spe1 primer pair and ligated to pFGL718 to give the intermediate clone p718-Ask1Up. Amplification of the *ASK1 ORF* 3' flanking region was carried out Ask1stop3UTRF-Hpa1/ Ask13UTRR-KpnI primers, digested with restriction enzymes and ligated

with HpaI/KpnI digested p718-Ask1Up to give p718-Ask1GFP (Fig. 3.9A).

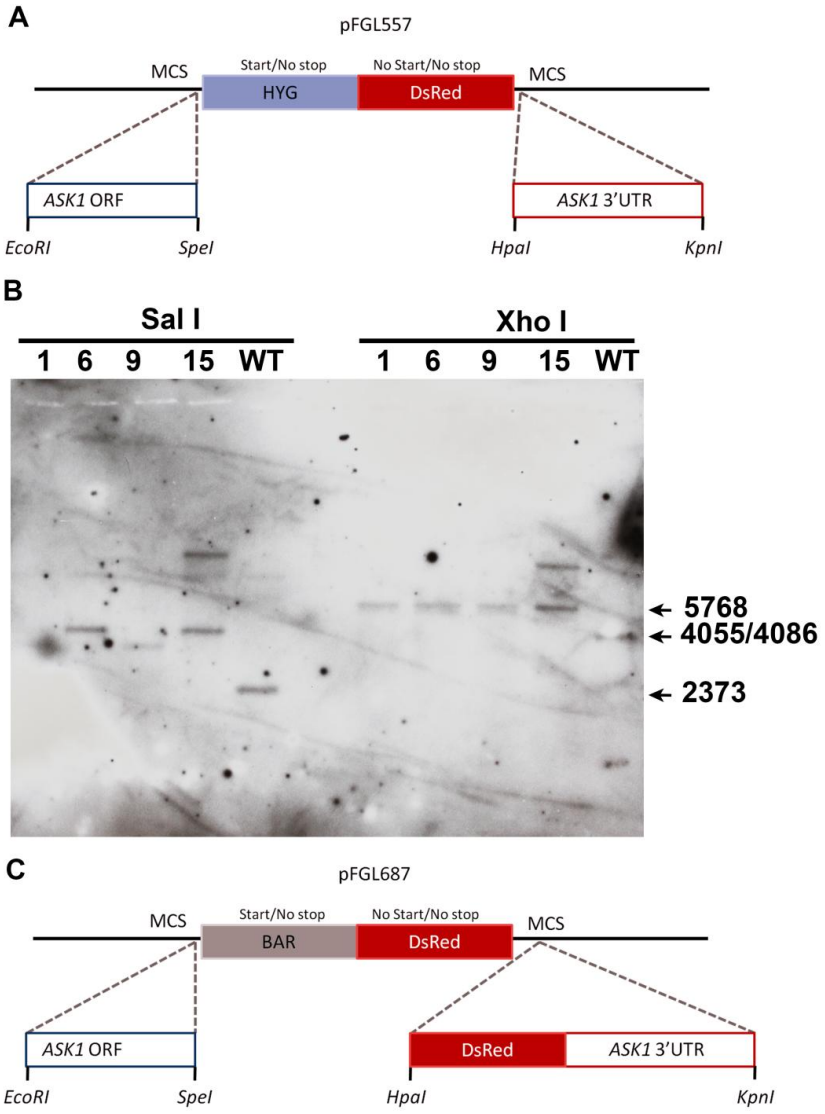

Figure 3.8: Generation of Ask1-DsRed tagged strain

A) Schematic diagram shows the marker-fusion tagging construct used for the replacement of the native *ASK1* locus with C-terminal DsRed-tagged *ASK1*. B) Southern hybridisation of genomic DNA, digested with SalI or XhoI, shows difference in fragment sizes between WT (SalI: 2 kb, XhoI: 4 kb) and *ASK1-DsRed* transformants (SalI: 4 kb, XhoI: 5.7 kb) consistent with correct integration at the native locus when probed with a fragment. C) Schematic diagram shows the marker-fusion tagging construct developed for the replacement of the native *ASK1* locus with C-terminal 2XDsRed-tagged *ASK1*.

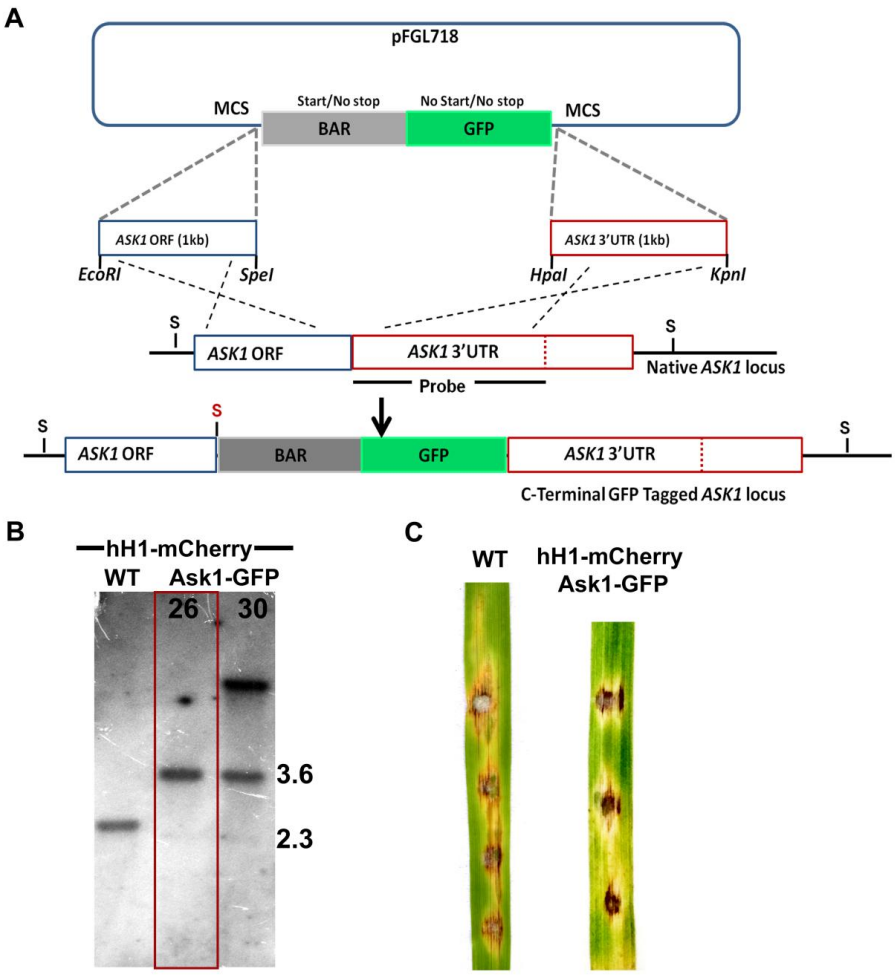

Figure 3.9: Strategy for generation and confirmation of Ask1-GFP tagged strains

A) Strategy used for replacement of the native *ASK1* locus with C-terminal GFP-tagged *ASK1* by marker-fusion tagging, S - SalI. B) Southern hybridisation of genomic DNA from the WT strain and *ASK1-GFP* transformants digested with SalI enzyme was probed with a fragment comprising the 3'UTR of *ASK1* confirmed single copy in-locus integration of *ASK1-GFP* cassette. The difference in fragment sizes between the *ASK1* (2.3 kb) and *ASK1-GFP* (3.6 kb) transformants is consistent with correct integration at the native locus. Transformants from B) with single copy integration were used for further analysis. C) Pathogenicity assay using drop inoculation of WT and *ASK1-GFP* tagged strains on detached barley leaves. The disease outcome was imaged 5 days post inoculation.

The constructs were verified by digestion with restriction enzymes. The plasmid was transformed into *M. oryzae* by ATMT and transformants were selected for resistance to glufosinate. The resistant transformants were screened by fluorescence microscopy and PCR, and confirmed by Southern hybridisation for site specific single integration (Fig. 3.9B). The transformants with single integration were tested for pathogenicity by drop inoculation on barley leaves. Five days post inoculation, the Ask1-GFP tagged strains induced infection symptoms similar to the WT (Fig. 3.9C).

Since Ask1, showed low fluorescence intensity with the DsRed tagging similar to Dam1, the localisation studies were all done with the C-terminal GFP-tagged Ask1 strain, Ask1-GFP. Though DsRed has been previously used for studies in *M. oryzae,* in my experience it is only suitable for more abundant proteins with stable localisation patterns (eg. histone, tubulin). It should not be the first tag of choice in cases where localisation patterns are not previously known or expected to be transient or dynamic (eg. DASH complex proteins).

Generation of GFP-tagged Mis12 strain

To track kinetochore dynamics in *M. oryzae*, I tagged Mis12, a subunit of the middle kinetochore MIS12 complex (MIND complex in budding yeast). Mis12, originally identified in *S. pombe* (Mtw1 in *S. cerevisiae*), connects the Knl1 complex and the Ndc80 complex, of the KMN network, to the CCAN through an interaction with the chromatin-associated CenpC and is essential for cell viability.

Mis12 is an approximately 30kDa protein (259 amino acids) that is associated with *S. pombe* and *S. cerevisiae* centromeres throughout the cell cycle and hence has often been used as a marker for the kinetochore in yeasts. C-terminal tagging of Mtw1 and Mis12 has been used in localisation studies and does not seem to affect the function of the protein.

In humans, Mis12 remains in the nucleus during interphase but does not bind to centromeres due to auto-inhibition.At the onset of mitosis, Aurora B phosphorylation relieves the inhibition to promote CenpC-Mis12 binding, thus laying the foundation for kinetochore assembly. SpMis12 appears as a single dot close to the SPBs during interphase until late G2, after which it was seen as 2-3 dots in mitosis as a short spindle assembled. ScMtw1 is seen as a single dot at the nuclear periphery in unbudded G1 cells. As a bud appears, Mtw1 is seen as two separate dots within a single nucleus, which segregate during anaphase.

Mis12 localisation patterns in *M. oryzae* would provide information about kinetochore dynamics, acting as a benchmark for the DASH complex protein dynamics. *Magnaporthe oryzae* Mis12 (MGG_06304) is a 398 amino acids protein with 32.3% similarity to *S. pombe* and 38.6% to *S. cerevisiae*. For C-terminal tagging of Mis12 (Fig. 10A), the *MIS12* 3' flanking region was amplified using primers Mis123UTRF-H3/ Mis123UTRR-Pvu1 from B157 genomic DNA and cloned into pFGL347 at HindIII/PstI to obtain pFGL347-Mis123'UTR. The last 1kb region from the 3' end of the *MIS12* ORF was amplified using primers Mis12orf-ER1/ Mis12cdsR-Sm1.

This fragment was then fused with the *GFP* ORF by PCR. The fusion product was cloned in pFGL347-Mis12 3'UTR at EcoRI/KpnI to give pFGL347-Mis12GFP. A similar construct was also developed for tagging of *MIS12* with mCherry. mCherry was PCR amplified from pFGL758 and fused with *MIS12* ORF as above. The Mis12-GFP construct was transformed into the H1-mCherry tagged strain by ATMT. The hygromycin resistant transformants were screened by PCR and fluorescence microscopy. Targeted replacement of native locus and single copy integration was confirmed by Southern hybridisation (Fig. 3.10B). All tagged strains were assessed for their virulence using drop inoculation of conidial suspension on detached barley leaves and were found to be pathogenic (Fig. 3.10C).

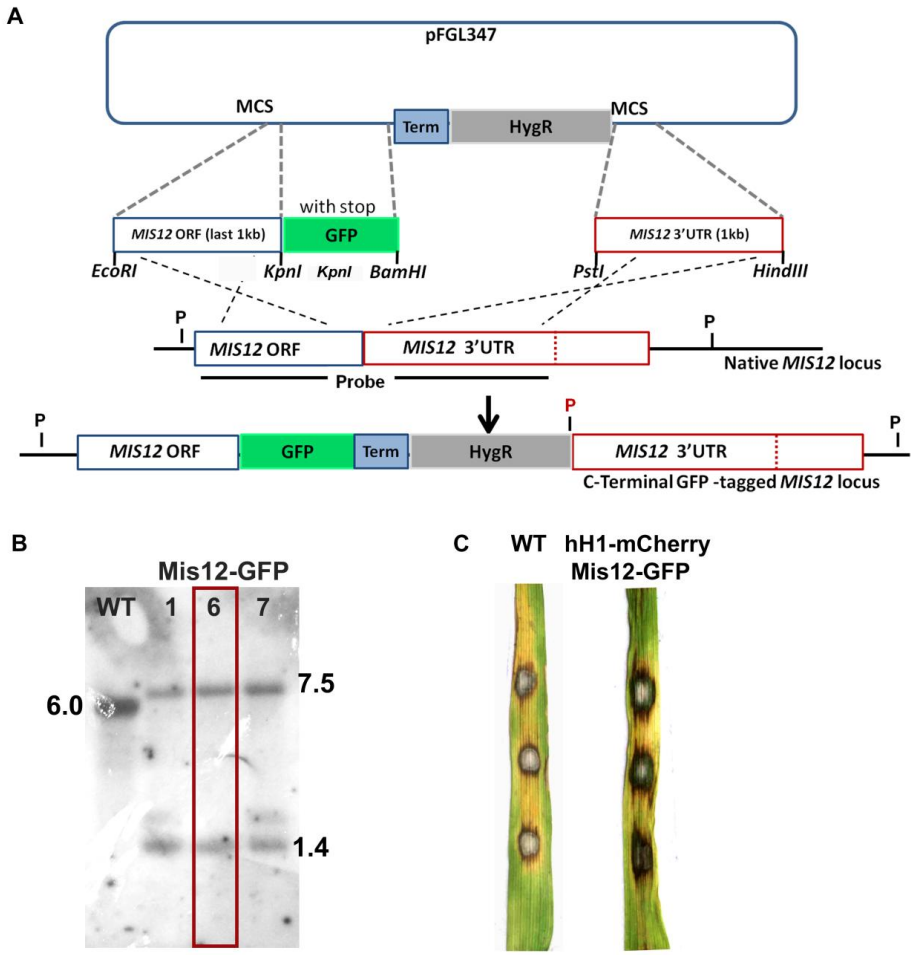

Figure 3.10: Generation of MIS12-GFP tagged strain

A) The strategy used for replacement of the native *MIS12* locus with C-terminal GFP-tagged *MIS12,* P - PstI. B) Southern hybridisation of genomic DNA digested with PstI showed a difference in fragment sizes between the WT (6 kb) and *MIS12-GFP* (1.4 and 7.5 kb) transformants, when probed with a fragment shown in A) comprising the last 1kb of ORF and 3'UTR of *MIS12*, which is consistent with correct integration at the native locus. Transformants from B), with single copy integration were used for further analysis. C) Pathogenicity assay using drop inoculation of WT and *MIS12-GFP* tagged strains on detached barley leaves. The disease outcome was imaged 5 days post inoculation.

Strains generated through this study are described in Table 3.2. Molecular biology protocols were followed as per laboratory manual (Sambrook and Russell, 2001). Table 3.3 provides nucleotide sequences of all primers used in the present study.

Generation of hH1-mCherry and β-tubulin-sGFP double tagged strain

The β-tubulin-sGFP tagging construct was derived from the pMF309 plasmid (a kind gift from Michael Freitag; (Freitag et al., 2004)). The β-tubulin-sGFP cassette was digested from pMF309 (10.4 kb), alongwith the upstream ccg1 promoter, with HpaI and SalI and ligated to KS-HPT (Hph resistance cassette in pBluescript KS+) at HpaI and XhoI to generate KS-HPT-β-tubulin:sGFP (9.2 kb) (Fig. 3.11A). The plasmid was confirmed by PCR and restriction enzyme digestion (Fig. 3.11B). Protoplast transformation was used to transfer the tubulin:sGFP tagging plasmid into the hH1-mCherry strain. Selection on hygromycin (Fig. 3.11C) recovered 24 resistant transformants which were screened for WT-like growth. The 7 positive transformants were further screened for fluorescence and the three positive transformants RGB3, RGB12 and RGB14 were screened by PCR and confirmed for β-tubulin:sGFP integration by Southern hybridisation (Fig. 3.11D, E). The double tagged RGB3, RGB12 and RGB14 strains were analysed for growth and pathogenicity on barley leaves (Fig. 3.11F). In case of RGB12, all these phenotypes were similar to the wild type (WT) B157 strain and it was used as a background strain for further study.

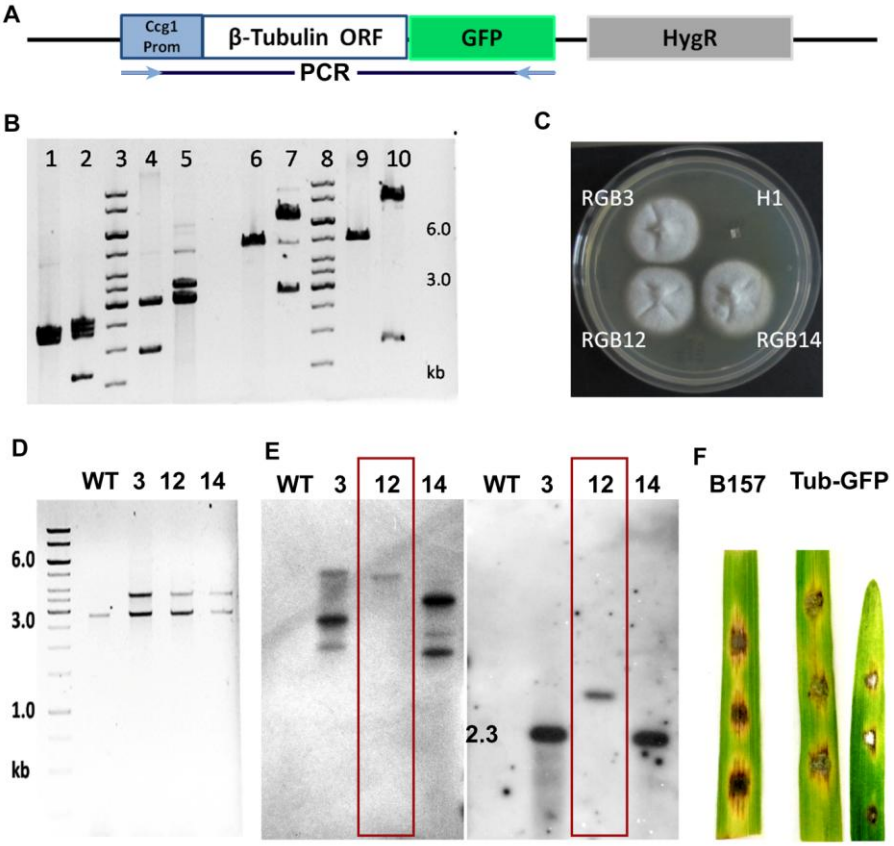

Figure 3.11: Generation of tubulin-GFP tagged strain via ectopic integration

A) Schematic diagram shows construct used for expression of *β-tubulin-sGFP* in *M. oryzae*. B) Confirmation of the tagging construct by restriction digestion. C) Screening of *β-tubulin-sGFP* transformants for hygromycin resistance. D) Screening of hygromycin resistant *β-tubulin-sGFP* transformants by PCR indicated in A). E) Southern hybridisation to confirm single copy integration of *β-tubulin-sGFP* construct. Genomic DNA from WT strain and β-tubulin-sGFP transformants was digested with NdeI or PvuII enzyme and the blot was probed with a fragment of the tubulin expression construct. F) Pathogenicity assay using drop inoculation of WT B157 strain and *β-tubulin-GFP* tagged strains on detached barley leaves. The disease outcome was imaged 5 days post inoculation.

3.2.2 Generation of mutant strains

While gene knock-out generally involves replacement of the gene of interest by a selectable marker, gene tagging involves the addition of a tag at the locus of interest. Both these strategies require targeted gene integration which is dependent on the inherent DNA repair mechanisms - non-homologous end joining (NHEJ) or homologous recombination (HR). While NHEJ is a non-specific, sequence independent repair system that ligates double stranded DNA breaks, HR involves recombination with a homologous template sequence. Like other filamentous fungi, the predominant repair mechanism in *M. oryzae* is NHEJ and as a result the average frequency of targeted gene integration is around 7%. (Villalba et al., 2008). However, this is locus specific, with certain locations showing upto 20% efficiency with 1 to 2 kb homology regions, while some others show extremely low frequencies. This low efficiency of gene targeting means screening a large number of transformants to identify true integrants, making the process laborious.

DNA binding proteins Ku80 and Ku70 form a heterodimer that recognises the double stranded breaks and recruits the NHEJ machinery. Inactivation of Ku80/Ku70 increases the efficiency of site specific integration without compromising the wild type phenotype in *Arabidopsis thaliana* and *Aspergillus nidulans*. A study in *M. oryzae* strains Guy11 and P1.2 where KU80 was knocked-out, reported an increase in targeted integration up to 80% without any defects in pathogenicity (Villalba *et al.*, 2008). Since the present work was carried out in the Indian isolate of *M. oryzae* B157, it was necessary to develop a NHEJ deficient version of this strain as a convenient tool for subsequent work.

Development of a strain for improved gene targeting in *M. oryzae*

1. *KU80* deletion in *M. oryzae* strain B157

The upstream and downstream 1-1.5kb flanking regions of *KU80* ORF were amplified from *M. oryzae* genomic DNA by PCR and cloned on either side of the Zeocin resistance cassette in pBS-KS^+ vector backbone (Fig. 12A). The KS-Moku80Δ::Zeo construct thus generated was moved into *M. oryzae* wild type strain B157 (WT) by protoplast transformation. The transformants were screened for targeted integration by PCR and confirmed by Southern Hybridisation (Fig. 3.12B-E). The confirmed *KU80* deletion strain, *ku80*Δ, was then used for further phenotypic characterisation.

2. Phenotypic characterisation of the *KU80* deletion strain, *ku80*Δ

The hyphal growth of the WT and *ku80*Δ strains was compared on oatmeal Agar (OMA) and they showed colony size comparable to the WT (Fig. 3.12F). Conidiation of *ku80*Δ was normal both in terms of morphology and number. Appressorium formation was assessed *in-vitro* on hydrophobic coverglass and morphology of spores, germ tube and appressorium was found similar to WT (Fig. 3.12G). Pathogenicity of WT and *ku80*Δ was determined by carrying out infection assay on 15 – 21 day old rice seedlings and both strains produced typical disease lesions 5 days post inoculation (dpi) (Fig. 3.12H). Thus *ku80*Δ did not show defects with respect to hyphal growth, conidiation, appressorium formation and rice infection and can be used as a background strain for subsequent studies to aid targeted integration by reducing the number of transformants to be screened in *M. oryzae* B157 strain.

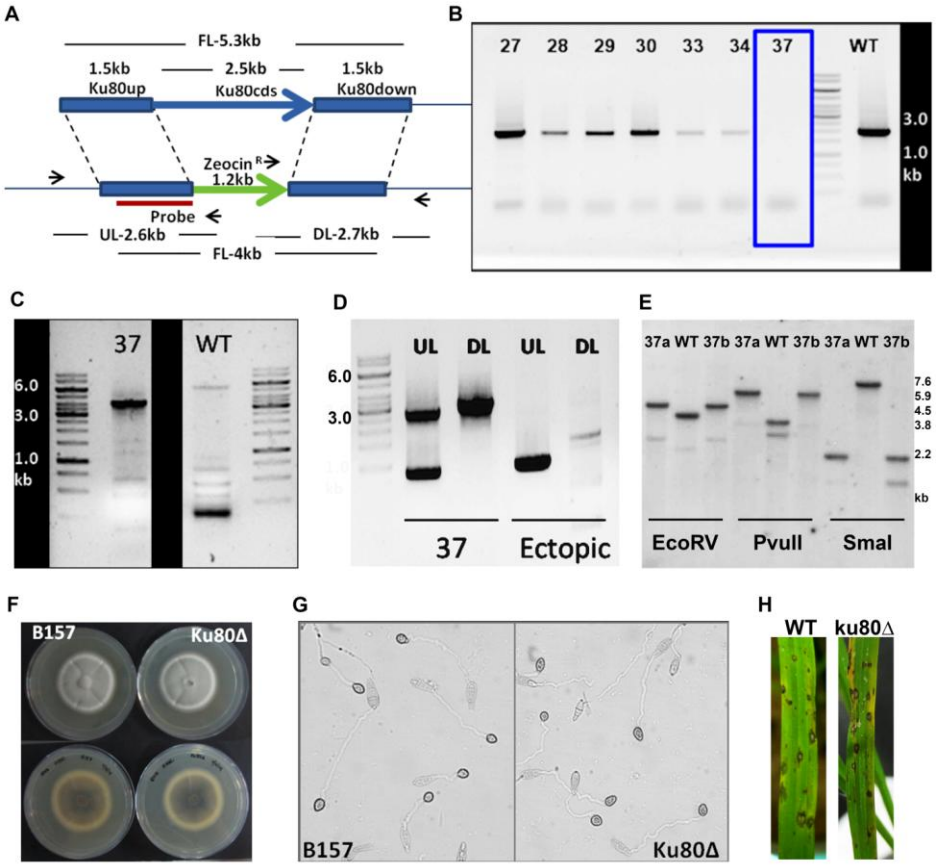

Figure 3.12: Generation of *KU80* deletion strain, *ku80*Δ

A) The strategy used for replacement of the native *KU80* locus with Zeocin resistance cassette. B) PCR based screening for amplification of *KU80* ORF. C) PCR based screening by amplification of full length *KU80* locus. D) Locus-specific PCR based screening by amplification of a fragment comprising of *KU80* flanking regions and Zeocin resistance cassette. E) Southern hybridisation of genomic DNA digested with EcoRV, PvuII and SmaI showed a difference in fragment sizes between the WT (EcoRV: 4 kb, PvuII: 3.8 kb and SmaI: 7.6 kb) and *ku80*Δ transformants (EcoRV: 4.5 kb, PvuII: 5.9 kb and SmaI: 2.2 kb), when probed with a fragment shown in A) comprising a fragment of the 5'UTR of *KU80*, which is consistent with correct integration at the native locus. Transformants from E) with single copy integration were used for further analysis. F) Vegetative hyphal growth of *ku80*Δ strain compared to WT on oatmeal agar. G) Appressorium formation in WT and *ku80*Δ strains on a hydrophobic surface. H) Pathogenicity assay using spray inoculation of WT and *ku80*Δ strains on 15-21 days old rice plants. The disease outcome was imaged 5 days post inoculation.

Generation of mutants of selected kinetochore genes

Representative genes, *CENPC*/*MIF2* from the inner, *MIS12*/*MTW1* from the middle and *DAM1* and *ASK1* from the outer KT complex were selected for study. KT proteins are essential in many systems studied. Functional analysis of these proteins has been done by use of temperature sensitive mutants and gene knock-down. Here, gene knock-down by RNA interference was chosen to study the role of *CENPC*, *MIS12* and *DAM1* in *M. oryzae*. *DAM1* has different roles in different fungal species. It was not known whether Dam1 is essential in *M. oryzae*, therefore, generation of deletion transformants was also attempted for *DAM1*.

Generation of knock-down transformants for *CENPC, MIS12 and DAM1*

Knock-down constructs were generated in pSilentDual-1 (pSD1) where a fragment of the gene of interest was cloned in between two promoters (TrpC and gpdA) placed in opposite orientation that allow transcription of both the strands and hence generate double stranded RNA. Recombinant plasmids were confirmed by PCR and restriction digestion (Fig 3.13B). The pSD1-CenpC, pSD1-Mis12 and pSD1-Dam1 plasmids were moved into *M. oryzae* RGB12 strain (WT; hH1-mCherry, β-tubulin-sGFP) by protoplast transformation. Transformants were selected for geneticin resistance.

The transformants showed reduced conidiation and appressorium formation (Fig. 3.13C, D). At transcript level, I observed *MIS12* and *DAM1* expression levels ranging from around 30-60% of the WT in the different silencing transformants. However, many of the CenpC and Mis12 silencing transformants were unstable, with frequent colony sectoring indicating growth and pigmentation heterogeneity, making it difficult to obtain consistent quantitative data (Fig. 3.13E). Many of the transformants were also difficult to revive from filter stocks. Knock down using a controllable or inducible siRNA expression, for example using TET On/Off promoters may be a better way of studying these genes.

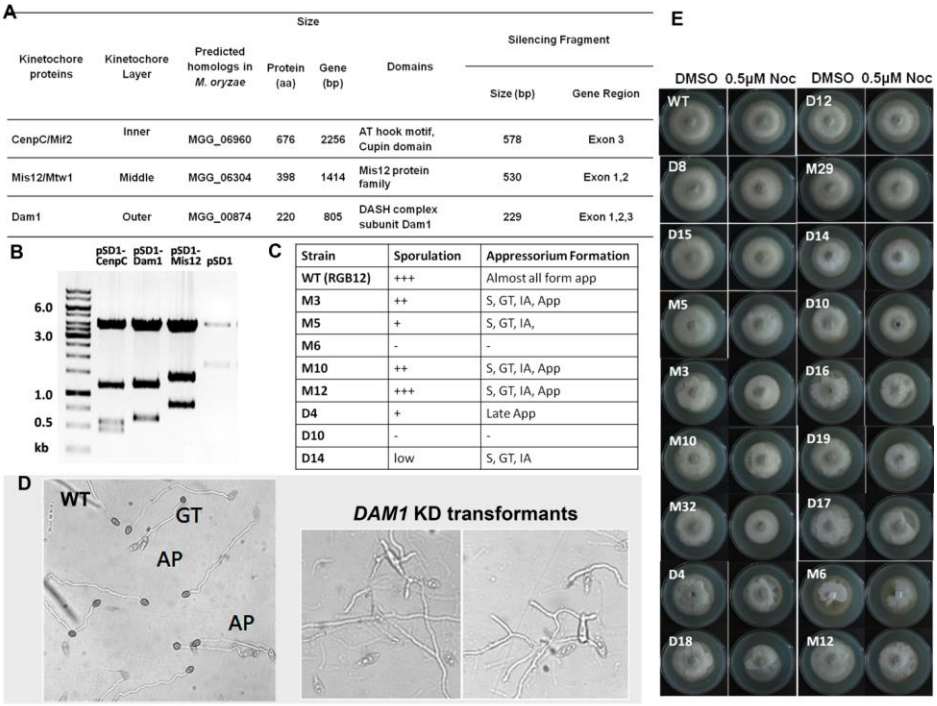

Figure 3.13: Knock-down transformants of kinetochore genes

A) Table provides details of *M. oryzae* kinetochore genes *CENPC*, *MIS12* and *DAM1*. B) Confirmation of *CENPC*, *MIS12* and *DAM1* silencing constructs by StyI restriction enzyme digestion. C) Summary of sporulation and appressorium formation defects of *MIS12* and *DAM1* knock-down transformants. D) Appressorium formation in WT and *DAM1* knock-down transformants on hydrophobic surface. E) Hyphal growth of WT and *MIS12* and *DAM1* knock-down transformants on DMSO (control) and nocodazole, observed 5dpi.

As a result these transformants were not used for further study and I focused only on the outer kinetochore proteins, proceeding next to the generation of the *DAM1* deletion mutant. In view of the phenotypes observed in the silencing mutants, I decided to carry out all Dam1 studies in the WT strains itself and not use the *ku80*Δ strain, in order to avoid any further complications that may arise due to the double deletion and so that the phenotypes can be solely attributed to Dam1.

Deletion of DASH complex genes *DAM1* and *ASK1*

Double-joint or overlap PCR was used to obtain the *DAM1* deletion cassette (Fig. 3.14A), such that upstream (972 bp) and downstream (530 bp) flanking regions were amplified from B157 genomic DNA and fused to the zeocin resistance cassette (1.24 kb). This deletion cassette was then cloned into an ATMT based plasmid to generate p718-DKO plasmid.

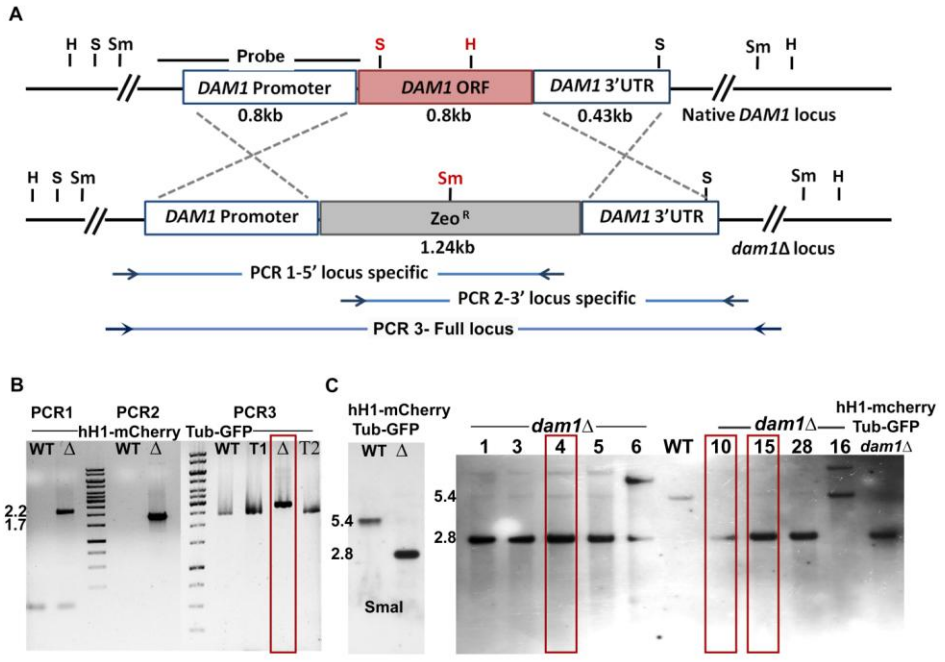

Figure 3.14: Generation of *dam1*Δ strains

A) Schematic diagram shows the strategy used for replacement of the *DAM1* gene with Zeocin resistance cassette, Sm - SmaI site. B) Screening of Zeocin resistant transformants by locus-specific PCR- 5' locus specific (PCR1), 3' locus specific (PCR2) and full-length locus PCR (PCR3). C) Southern hybridisation of *dam1*Δ transformants confirmed deletion of *DAM1* by single copy targeted integration of Zeocin resistance cassette. Genomic DNA digested with SmaI (Sm) and probed with a fragment comprising the *DAM1* promoter region marked in A) showed a difference in fragment size between the WT (5.4 kb) and *dam1*Δ transformants (2.8 kb) consistent with correct replacement of the *DAM1* ORF.

The construct was transformed into WT B157 strain and the histone, tubulin dual tagged strain to obtain *DAM1* mutants. Zeocin resistant transformants were screened by amplification of *DAM1* ORF and confirmed by locus specific PCR (Fig. 3.14B). Correct deletion of the *DAM1* ORF was confirmed by Southern hybridisation (Fig. 3.14C). Once the DAM1 deletion mutant was obtained, the silencing transformants were not used further in order to obtain clearer data and all phenotypic assays were carried out using this deletion mutant.

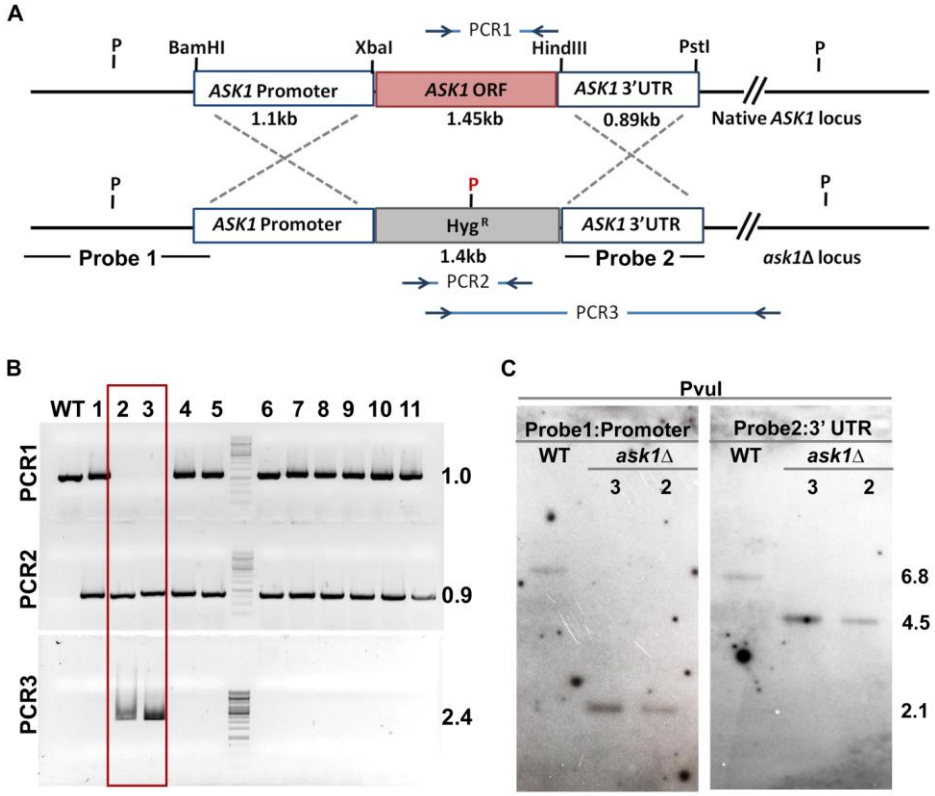

Figure 3.15: Generation of *ask1*Δ strain

A) Schematic diagram shows the strategy used for deletion of the *ASK1* ORF by replacement with *HPH* cassette, P - PvuI site. B) Screening of the hygromycin resistant transformants by PCR for various regions marked as PCR1, PCR2 and PCR3 in A). C) Southern hybridisation of transformants confirmed deletion of the *ASK1* gene by single copy targeted integration of the *HPH* cassette. The difference in fragment sizes between the WT (6.8 kb) and *ask1*Δ transformants (2.1 or 4.5 kb) genomic DNA digested with PvuI (P) and probed with the fragments marked in A) is consistent with correct replacement of the *ASK1* ORF.

For *ASK1* deletion (Fig. 3.15), the 1080 bp upstream and 889 bp downstream flanking regions of the *ASK1* ORF were cloned upstream and downstream of the hygromycin resistance cassette respectively in an ATMT based vector (Fig. 3.15A). The vector was transformed into the GFP-Dam1 strain by ATMT and selected for hygromycin resistance.

The hygromycin resistant transformants were screened by several different PCRs (Fig. 3.12B). PCR1 involves amplification of a fragment of the *ASK1* ORF, seen as a ~1kb fragment in the WT strain and ectopic transformants and absent in deletion mutants (Fig 3.15B). PCR2 is amplification of the hygromycin phosphostransferase *ORF* (0.9 kb), observed positive in transformants and absent in the WT strain. PCR3, a locus-specific PCR that amplifies the integration junction, is composed of the hygromycin resistance cassette as well as the *ASK1* flanking region, and is positive only in true site specific integrants and absent in the WT and ectopic transformants (Fig. 3.15B). Correct deletion of the *ASK1* ORF and single integration of cassette was confirmed in the PCR positive transformants selected from (B) by Southern hybridisation using probes binding to the upstream and downstream flanking regions marked in (A) (Fig. 3.15C).

Development of *dam1*Δ complementation strain

Complementation of the *dam1*Δ strain was carried out using the N-terminal GFP-Dam1 construct (p718-GFP-Dam1) developed earlier for studying Dam1 protein dynamics (Fig. 3.16A). The plasmid was transformed into *dam1*Δ strain by ATMT and selected for glusfosinate (bialaphos) resistance. The glufosinate resistant transformants that showed WT-like growth were screened by PCR (Fig. 3.16B). Southern hybridisation was used to determine the number of integrations in each strain and identify strains with a single copy of the *DAM1* construct (Fig. 3.16C). Several transformants with 1 or 2 copies of the DAM1 expression construct were obtained. Transformants 12, 16 and 30 with a single *DAM1*

copy and 1-5 and 2-6 (two copies) were selected for phenotypic characterisation.

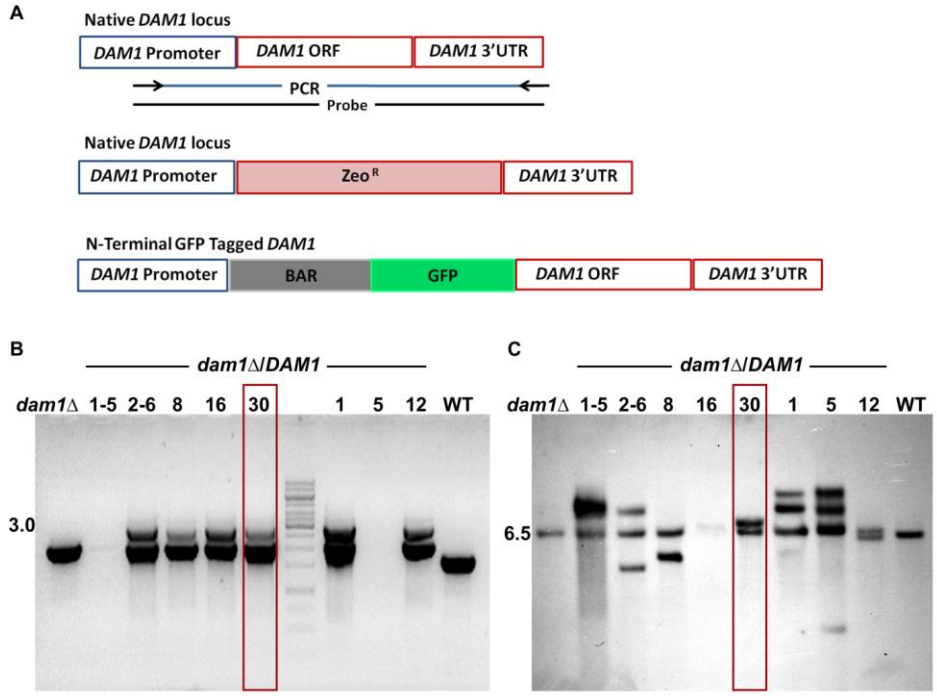

Figure 3.16: Complementation of *dam1*Δ strain with GFP tagged *DAM1*

A) Schematic diagram shows the *GFP-DAM1* construct used for complementation of *dam1*Δ strain. B) Screening of bialaphos resistant transformants by *DAM1* locus PCR marked in A). C) Southern hybridisation of transformants to confirm integration of single copy of *DAM1* gene. Genomic DNA from *dam1*Δ, complementation transformants *dam1*Δ/*DAM1* and WT strain was digested with KpnI and the blot was probed with a fragment comprising the *DAM1* locus as indicated in A). PCR and Southern hybridisation showed that the complementation construct was inserted at an ectopic location.

The complementation transformants were analysed for vegetative hyphal growth (colony diameter), conidiation and pathogenic development. Although no differences were apparent in the phenotypes between the transformants varying in copy numbers, data is shown only from the single copy integrants.

Table 3.2: List of fungal strains developed in the study

Strain	To study	Description
hH1-mCherry	Chromosomes and nucleus	C-terminal mCherry-tagged histone H1 inserted at ILV2 locus in WT
β-Tub-GFP	Microtubule network	C-terminal GFP-tagged β-tubulin, random integration in WT
hH-mCherry β-Tub-GFP WT (RGB12)	Nuclear and spindle organisation	C-terminal GFP-tagged β-tubulin in hH1-mCherry strain
GFP-Dam1	Localisation of Dam1	N-terminal GFP-tagged Dam1 in WT
DsRed-Dam1	Localisation of Dam1	N-terminal DsRed-tagged Dam1 at native locus in WT
Ask1-DsRed	Localisation of Ask1	C-terminal DsRed-tagged Ask1 at native locus
hH1-mCherry, GFP-Dam1	Localisation of Dam1 relative to chromosomes	N-terminal GFP-tagged Dam1 at native locus in hH1-mCherry strain
hH1-mCherry, Ask1-GFP	Localisation of Ask1 relative to chromosomes	C-terminal GFP-tagged Ask1 at native locus in hH1-mCherry strain
hH1-mCherry, Mis12-GFP	Localisation of Mis12 relative to chromosomes	C-terminal GFP-tagged Mis12 at native locus in hH1-mCherry strain
*dam1*Δ	Effect of loss of Dam1 on fungal infection cycle	*DAM1* locus replaced by Zeocin resistance cassette in WT
*dam1*Δ	Effect of loss of Dam1 on mitosis	*DAM1* locus replaced by Zeocin resistance cassette in RGB12
*ask1*Δ	Effect of loss of Ask1	*ASK1* locus replaced by Hygromycin resistance cassette
*dam1*Δ/ GFP-Dam1	To complement defects due to loss of Dam1	Complementation of *dam1*Δ with GFP-Dam1
*ku80*Δ	To increase efficiency of targeted integration	*KU80* locus replaced by Zeocin resistance cassette

Table 3.3: List of Primers used in the study

Primer	Sequence (5'- 3')
N-Terminal tagging of Dam1 by MFT	
Dam1-Pro-F	GAGAGTGTTgaattcCCGCCAATAGATCGACACAT
Dam1-Pro-R	GAGAGTGTTgtcgacTGATGGTTTTGCTCGTTTTGG
Dam1-ORF-F	GAGAGTGTTcccgggAATGGCAACCCGCGACGAA
Dam1-3UTR-R	GAGAGTGTTggtaccGTGGCTGAAGATTCCCCAAG
C-Terminal tagging of Mis12	
Mis12orf1kbF-E1	GAGAGTGAgaattcCCCCAGTCGAAAAAGACAAA
Mis12cdsR	AGGCTCGTCCATGGCATC
VenusF-Mis12OH	GATGCCATGGACGAGCCTATGGTGAGCAAGGGCGAGGAG
VenusR-KpnI	GAGAGTGTTggtaccCTACTTGTACAGCTCGTCCATG
Mis12UTRF-PstI	GAGAGTGTTctgcagCTGTGATGTGTCGGCCTATG
Mis12UTRR-H3	GAGAGTGAaagcttGTGGGCCGAGAGGTACAATA
C-Terminal tagging of Ask1 by MFT	
Ask1tagcdsF-ER1	GAGAGTGAgaattcCCATAGTCACGGCTCCTGAT
Ask1tagcdsR-Spe1	GAGAGTGAactagtAAAAGAATCGTCCAGGATGTTG
Ask13UTRF-Hpa1	GAGAGTGTTgttaacAGGCACAAGGTGGTCAAGAT
Ask1stop3UTRF-Hpa1	GAGAGTGTTgttaacTGAAGGCACAAGGTGGTCAAGAT
DAM1 deletion	
Dam1_Up_F	GATGCTCCATAGTCCTTCAC
Dam1_Up_R	ctccttcaatatcagttaacgtcGGGAATGAGTGACGTGGAT
Dam1_Down_F	gaaaattccgtcaccagccctggGTTTCTGGATGGTGGCAGAT
Dam1_Down_R	CAGTTCCAAGGTGCTGTT
ASK1 Deletion	
Ask1KOUpF-BH1	GAGAGTGAggatccACAACTCCACCCAAAACTGC
Ask1KOUpR-Xb1	GAGAGTGTTctagaCTGGTTGTTTGCCTGGTTTT
Ask1KODnF-PstI	GAGAGTGTTctgcagAGGCACAAGGTGGTCAAGAT
Ask1KODnR-H3	GAGAGTGAaagcttCGTCAGCAATGATGGAAATG
Silencing of *CENPC*, *MIS12* and *DAM1*	
CenpC_si_F	CTAGTCTAGACCCCTTTCACTGCTTGCTA
CenpC_si_R	CCCAAGCTTGCTTCTTGGCGATTGGAG
Mis12_si_F	CATTGCGCCGACTCAAGTATC
Mis12_si_R	CCTGCCAATTTCATCCTTTTG
Dam1_si_F	GGCAGATGGAGGAGAATCAG
Dam1_si_R	CCCAAGCTTCCCGAGGATGATGCTCTACC
KU80 Deletion	
Ku80KO1	GCCATGAGGTCTGATATACCC
Ku80KO2	CAC*AAGCTT*GGGGGTCTGACGGGTTCTGG
Ku80KO3	GTG*GAATTC*CACGAGCTGCTTAATGCTGGGC
Ku80KO4	CGGTCAGCAACTCGCTGG
Ku80uplocus	GGCAGCTCGGCACGAAACG
Ku80downlocus	CATGCTGACCGTTCGTGGCC
Ku80cdsF	CCATACAAGATGGCTGAC
Ku80cdsintR	CACTCTCCTTGTATGTCTC